

RESEARCH ARTICLE

**Preservation of Truncal Genomic Alterations in Clear Cell and Papillary
Renal Cell Carcinomas with Sarcomatoid Features: An Intra- and
Intertumoral, Multifocal Fluorescence *in Situ* Hybridization Analysis Reveals
Limited Genetic Heterogeneity[†]**

Running Head: Genetic Heterogeneity in Sarcomatoid RCC

**Joseph M. Sanfrancesco¹, John N. Eble¹, David J. Grignon¹, Mingsheng Wang¹, Shaobo
Zhang¹, Chandru P. Sundaram², Muhammad T. Idrees¹, Roberto Pili³, Erik Kouba¹, Liang
Cheng^{1,2}**

From the Departments of Pathology and Laboratory Medicine¹, Urology², and Medicine³,

Indiana University School of Medicine, Indianapolis, Indiana, USA.

Address correspondence and reprint requests to Liang Cheng, M.D., Department of Pathology
and Laboratory Medicine, Indiana University School of Medicine, 350 West 11th Street, IUHPL
Room 4010, Indianapolis, IN 46202, USA. Telephone: 317-491-6442; Fax: 317-491-6419;
E-mail: liang_cheng@yahoo.com

[†]This article has been accepted for publication and undergone full peer review but has not been
through the copyediting, typesetting, pagination and proofreading process, which may lead to
differences between this version and the Version of Record. Please cite this article as doi:
[10.1002/mc.22699]

Received 15 February 2017; Revised 19 June 2017; Accepted 29 June 2017
Molecular Carcinogenesis
This article is protected by copyright. All rights reserved
DOI 10.1002/mc.22699

This is the author's manuscript of the article published in final edited form as:

Sanfrancesco, J. M., Eble, J. N., Grignon, D. J., Wang, M., Zhang, S., Sundaram, C. P., Idrees, M. T., Pili, R., Kouba, E. and Cheng, L. (2017), Preservation of Truncal Genomic Alterations in Clear Cell and Papillary Renal Cell Carcinomas with Sarcomatoid Features: An Intra- and Intertumoral, Multifocal Fluorescence *in Situ* Hybridization Analysis Reveals Limited Genetic Heterogeneity. *Mol. Carcinog.*. Accepted Author Manuscript.

<http://dx.doi.org/10.1002/mc.22699>

Abstract

Understanding tumor genomic heterogeneity may offer vital information in an age of targeted therapy for renal cell carcinoma. We sought to investigate hallmark truncal chromosomal alterations between conventional, sarcomatoid, and matched metastatic tumor foci in clear cell and papillary renal cell carcinomas. A retrospective review identified 58 cases including clear cell (CCRCC) and papillary renal cell carcinomas (PRCC). All cases contained sarcomatoid transformation. Additionally, 10 of 58 patients had matched metastatic disease available for analysis. Three separate foci of conventional and sarcomatoid morphologies were analyzed in each tumor using dual color interphase fluorescence in situ hybridization. In the CCRCC cohort, hallmark chromosome 3p deletion was identified in 71% of cases (37/52). Complete concordance of chromosomal status between intratumoral foci in sarcomatoid and conventional foci was 89% and 86%, respectively. Overall chromosome 3p status between matched conventional and sarcomatoid morphologies was identified in 98% of cases (51/52). Hallmark 3p deletion was present in 91% of CCRCC metastatic samples (10/11) and was concordant with the matched primary CCRCC tumor in 91% (10/11). In the PRCC cohort, trisomy 7 and 17 was identified in all six cases (6/6). Complete concordance between intratumoral foci of trisomy 7 and 17 was 83% (5/6). Trisomy 7 and 17 were identified in all metastatic PRCC samples with 100% concordance with the matched primary tumor. These data show the relative preservation of truncal chromosomal abnormalities between conventional and sarcomatoid morphologic as well as matched metastatic settings. This article is protected by copyright. All rights reserved

Keywords: Kidney; sarcomatoid renal cell carcinoma; fluorescence in situ hybridization (FISH); molecular genetics/cytogenetics; targeted therapy; precision medicine; differential diagnosis

Introduction

The morphological and genetic complexities of renal cell carcinoma (RCC) have been extensively studied. Additionally, several recent studies have used genomic sequencing to highlight intratumoral genetic heterogeneity.[1-6] Such complexities are compounded by the predisposition of a subset of RCC to undergo sarcomatoid differentiation. RCC with sarcomatoid features, regardless of the conventional morphologic subtype, has been shown to be associated with an overall worse prognosis.[7] Accordingly, studies have attempted to characterize the extent of intratumoral heterogeneity within sarcomatous tumor components and compare the differences between conventional (e.g. epithelial) and sarcomatous elements.[8,9]

Intratumoral genetic heterogeneity, particularly in the setting of divergent morphologic features and/or high clinical stage, may have significant impact on treatment options for patients, especially those with metastatic disease[10]. Hallmark chromosomal gains and losses in primary RCC have been characterized, most notably the presence of chromosome 3p deletion in clear cell RCC (CCRCC) and trisomy 7 and 17 in papillary RCC (PRCC)[11-20]. Prior studies have attempted to compare intratumoral concordance of hallmark chromosomal gains and losses and subsequent concordance with matched metastases.[21-23] We herein investigate the preservation of hallmark chromosomal abnormalities along with intratumoral concordance in the setting of matched sarcomatous transformation and matched metastatic disease in CCRCC and PRCC.

Materials and Methods

Fifty-eight patients diagnosed with either CCRCC (52 patients) or PRCC (6 patients) with sarcomatoid transformation between 1995 and 2016 were retrieved from our institution's surgical pathology files. Histopathologic features of each case were evaluated by a single senior

genitourinary pathologist (LC) and confirmed using diagnostic criteria set forth in the World Health Organization Classification of Tumors of the Urinary System and Male Genital Organs.[24] Appropriate sections containing both conventional and sarcomatoid tumor foci were selected for subsequent analysis. Specimens of biopsy/resection-proven metastatic tumors of the patients were also identified and lesions were matched with primary lesions for analysis. This study was approved by the Institutional Review Board.

Formalin-fixed, paraffin-embedded tissue blocks of each tumor were obtained based on correlation with the reviewed hematoxylin and eosin-stained glass slides demonstrating conventional (epithelial) and sarcomatoid morphologies. Three separate foci of conventional and sarcomatoid morphologies were analyzed in each primary tumor. When available, three foci of metastatic RCC were marked, analyzed, and compared to their primary RCC (**Figure 1**).

Fluorescence in situ hybridization (FISH) analysis was performed on each of these selected foci to identify the presence of hallmark chromosomal abnormalities associated with CCRCC and PRCC including deletion of 3p and trisomy 7 and 17, respectively, as described previously.[25,26]

Selected slides were deparaffinized with two washes of xylene, 15 min each; washed twice with absolute ethanol, 10 min each; and air-dried in a fume hood. Subsequently, the slides were treated with 0.1mM citric acid (pH 6.0) at 95 degrees for 10 min, rinsed in distilled water for 3 min, and followed by a wash of standard saline citrate ($2 \times$ SSC) for 5 min. Tissue digestion was performed by applying 0.4 ml of pepsin (Sigma, St. Louis, MO, USA) solution (4 mg/ml in 0.9% NaCl in 0.01N HCl) to each slide and incubating the slides in humidified box for 40 min at 37 °C. The slides were rinsed with distilled water for 5 min, washed with SSC for 5 min, and air-dried.

The alterations in chromosomes 7 and 17 were assessed using a probe cocktail containing probe CEP7 (green) and CEP17 (orange). The CEP7/CEP17 probe set was diluted with tDenHyb1 (Insitus, Albuquerque, NM, USA) in ratios of 1:50 and 1:100, respectively. Deletion of chromosome 3p was assessed using a probe cocktail containing BAC clone probe to chromosome 3p25 (RP11-572 M14, Green; Empire Genomics, Buffalo, NY, USA) and CEP3 (CEP3-Orange; Abbott, Downers Grove, IL, USA). The VHL gene was mapped at 3p25.3 (chr3:10,141,008-10,153,670). The BAC clone RP11-572M14 (chr3: 10,011,785-10,180,797) covers 100% of the gene VHL. The 3p25/CEP3 probe set was diluted with tDenHyb2 (Insitus) in ratios of 1:50. The diluted probe (5 μ l) was applied to each slide under reduced light conditions. The slides were then covered with a 22 \times 22 mm coverslip and sealed with rubber cement. Denaturation was achieved by incubating the slides at 83 $^{\circ}$ C for 10 min in a humidified box and hybridization at 37 $^{\circ}$ C overnight. The coverslips were removed, and the slides were washed twice with 0.1 \times SSC/1.5 M urea at 45 $^{\circ}$ C (20 min for each), followed by a wash with 2 \times SSC for 20 min, and with 2 \times SSC/0.1% NP-40 for 10 min at 45 $^{\circ}$ C. The slides were further washed with 2 \times SSC at room temperature for 5 min. The slides were air dried and counterstained with 10 μ l 4,6-diamidino-2-phenylindole (Insitus), covered with coverslips, and sealed with nail polish.

The hybridized slides were observed and documented using a MetaSystem FISH system (MetaSystem, Newton, MA, USA) under \times 100 oil objective. The images were acquired with a cool box camera and analyzed with MetaSystem Isis software (MetaSystem). The following filters were used: SP-100 for DAPI, FITC MF-101 for spectrum green, and Gold 31003 for spectrum gold signals. Signals from each color channel (probe) were counted under false color, with computerized translation of each color channel into blue, green, and red. Four sequential

focus stacks with 0.3- μ m intervals were acquired and integrated into a single image to reduce thickness-related artifacts.

Analysis was performed identifying 100–150 nuclei from tumor tissue for each slide and was scored for probe signals under the fluorescence microscope with $\times 1000$ magnification[16,27]. Definitions of chromosomal trisomy for chromosomes 7 and 17 were based on the Gaussian model and were related to the nonneoplastic renal cortex control cell signals. The cutoff values were set for each probe at the mean plus 3 standard deviations of the control values. The method of analysis for 3p25 deletion was based on previous studies of chromosome deletions at 1p and 19q in oligodendrogliomas. The cutoff value for 3p deletion was defined as a 3p25/CEP3 ratio of ≤ 0.7 . Chromosome 3p deletion was considered to be characteristic of CCRCC and trisomy of chromosomes 7 and/or 17 was considered characteristic of PRCC.

Results

We identified 58 patients with CCRCC (n=52) or PRCC (n=6) tumors with sarcomatoid features, additionally 13 samples (CCRCC n = 11; PRCC n = 2) of metastatic disease from 10 different patients were available for comparative analysis to the primary tumor. All tumors were the International Society of Urological Pathology (ISUP; formerly Fuhrman) nuclear/nucleolar grade 4 of 4. The male-to-female ratio was 1.5:1 and the mean age was 57 years at the time of the primary resection (median, 57; range, 28–77 years). The degree of sarcomatoid features in the primary tumor ranged from <5–90%. Primary renal tumor sizes ranged from 2.0–20.5 cm and metastatic sites included lymph nodes, bone, gastrointestinal tract, lung, brain, and liver. A chromosomal aberration in at least one tumor focus was considered adequate to classify a

morphologic component as deletion (e.g., chromosome 3p) or polysomy (e.g., chromosome 7/17).

Clear Cell Renal Cell Carcinoma

The study cohort of CCRCC with sarcomatoid features included 52 patients with a male-to-female ratio of 1.3:1 and mean and median ages of 57 and 59 years, respectively. The primary tumor sizes ranged from 4.3–20.5 cm (mean, 10.6 cm). Pathologic stages of primary tumors (when available) were T1b (n=3), T2a (n=1), T2b (n=2), T3a (n=30), T3b (n=2), and T4 (n=4). The percentage of sarcomatoid features in the primary CCRCC tumors ranged from <5–90%. Eleven metastatic tumor site samples from 8 different patients were available for comparison to their primary CCRCC including bone (n=3), brain (n=2), gastrointestinal (n=2), liver (n=2), lymph node (n=1), and lung (n=1) [**Table 1**].

Of the 52 CCRCC with sarcomatoid features, chromosome 3p deletion was identified in 71% of cases (37/52) (**Figure 2**). When chromosomal alterations between the 3 selected sarcomatoid tumor foci were compared, complete concordance of chromosome 3p deletion in all 3 foci was identified in 32 of 37 cases (86%). Three of the remaining cases with chromosome 3p deletion demonstrated absence of deletion at a single focus within the sarcomatoid component and 2 cases showed absence at 2 of 3 foci. In comparison, the 3 selected conventional CCRCC tumor foci showed complete concordance of hallmark chromosome 3p deletion in 31 of 36 cases (86%). Three of the remaining cases with chromosome 3p deletion demonstrated absence of a deletion in a single tumor focus with the final 2 cases showing absence of 3p deletions at 2 of 3 foci. Complete concordance between conventional clear cell and sarcomatoid morphologies of lesions was identified in 81% of cases (42/52); however, concordance of overall chromosome 3p

status (including concordant and discordant 3p deletions) between the morphologic components was 98% (51/52) (**Figure 3**). Only one case demonstrated absence of chromosome 3p deletion in all 3 foci of conventional CCRCC while demonstrating 3p deletion in all 3 sarcomatoid foci. Hallmark 3p deletion was present in 91% of CCRCC metastatic samples (10/11). Metastases showed 91% (10/11) concordance between matched primary conventional and sarcomatoid tumor foci (**Figure 4**). Of note, one case demonstrated an absence of 3p deletion in all 3 metastatic foci compared to the primary tumor. Importantly, all 11 metastatic lesions showed complete concordance between all 3 tumor foci.

Papillary Renal Cell Carcinoma

The study cohort of PRCC with sarcomatoid features included 6 patients with a male-to-female ratio of 5:1 and mean and median ages of 54 and 56 years, respectively. The primary tumor sizes ranged from 2.0–15 cm (mean, 7.1 cm) and pathologic stages of primary tumors were T1a (n=1), T2a (n=2), and T3a (n=3). The percentage of sarcomatoid features in the primary PRCC tumors ranged from <5–60%. Corresponding specimens of metastatic disease were identified in 2 patients and the sites included small bowel (n=1) and lung (n=1) [**Table 1**].

Trisomy 7 and 17 were identified in 100% (6/6) of PRCC tumors with sarcomatoid features. When comparing chromosomal alterations between the 3 selected sarcomatoid tumor foci, complete concordance was identified in 83% (5/6) of cases (**Figure 5**). A single focus in one case demonstrated disomy 7 and 17 within the sarcomatoid component. In comparison, findings among the 3 selected conventional PRCC tumor foci showed complete concordance in 83% (5/6) of cases. Again, a single focus in one case demonstrated disomy 7 and 17. The overall concordance of matched sarcomatoid and conventional features in the PRCC cohort was 100%

(6/6). Trisomy 7 and 17 was present in all PRCC metastases (2/2) and showed 100% concordance with primary conventional and sarcomatoid tumor foci (**Figure 6**).

Discussion

In this study, we evaluated the presence and maintenance of truncal chromosomal aberrations of multiple tumor foci in matched conventional and sarcomatous components of primary RCC. CCRCC is the most common RCC subtype and mutations of von Hippel Lindau gene (*VHL*) and the loss of chromosome 3p are fundamental events in development.[13,14,28] Previously, discordant 3p deletion patterns have been shown in multifocal CCRCC (intrarenal metastatic spread)[26]; however, Gerlinger et al have demonstrated preservation of chromosome 3p deletion sampling multiple regions of 10 CCRCC cases.[4] Our study includes 58 different patients and considering the multifocal sampling performed, we were able to evaluate the chromosomal status of 374 primary tumor foci. With 13 samples of metastatic tumor from 10 of 58 patients, our total foci for comparison became 387. While recent studies have highlighted variations in the subclonal population identified by genomic sequencing, our multifocal intra- and intertumoral evaluation of hallmark chromosomal aberrations serves to highlight impressive concurrence of chromosomal status in the setting of divergent morphology and metastasis.[29]

Sarcomatoid divergence in RCC is associated with aggressive behavior, high pathologic/clinical stage, and overall poor prognosis.[7] Approximately 5–10% of RCC have some component of sarcomatoid morphology.[7] The underlying mechanisms of transition to sarcomatoid differentiation have been extensively hypothesized; however, regardless of such purported mechanisms causing this divergence, limited prior study shows chromosomal aberrations of the conventional components appear to be maintained.[30] Prior landmark

genomic studies in RCC subtypes typically excluded cases with divergent morphology, which explains the paucity of data evaluating preservation of these recurrent chromosomal aberrations in the setting of sarcomatoid differentiation [9].

Cancer evolution remains an extensively studied concept and encompasses a complicated series of molecular events. While hypotheses and opinions differ, it appears that RCCs arise from a single clonal event which subsequently branch (or “braid”) into subclonal events. A key point of contention is how these subclones interact, if at all, as the tumor evolves [17,20,31]. Herein lays the debate between linear versus braided evolution from a truncal event in tumorigenesis.[32] Furthermore, the “braided” model hypothesizes that spatially heterogeneous mutations may happen at different points in time but the overall genomic profile inevitably becomes similar [33]. Given that many subclones are point mutations or short segment gains and losses, FISH study methodology is crucial. Analytical resolution of FISH is determined by probe size and labeling methods[16]. By using plasmid or oligo probes, detection could increase resolution to 2-3 KB level. These types of probes are especially useful for the detection of micro-deletions but with reduced sensitivity. It is still unclear how these small genetic lesions interact with clinical tumor progression or contribute to possible resistance to treatment.[21] Regardless, many of these subclones, while being genetically distinct, do share identical driver mutations [29,34,35].

Regardless of the role of subclones in tumor evolution, chromosome 3p abnormalities in CCRCC and trisomy 7/17 in PRCC remain significant in tumorigenesis and targeted treatment [8,25]. In CCRCC, these abnormalities directly relate to the *VHL* gene, which is located at 3p25. Variations in *VHL* expression have direct consequences to three key pathways including the hypoxia-inducible factor (*HIF*), mammalian target of rapamycin (*MTOR*), and overexpression of

Accepted Article

vascular endothelial growth factor/platelet-derived growth factor (VEGF) [14,17,22,32]. *VHL* is a ligase responsible for degrading *HIF1/2A*. Given the vascular nature of CCRCC, the angiogenesis seen in these lesions is likely a direct result of this uninhibited activation.[36] The importance of chromosome 3p deletion and *VHL* genetic alterations stems from their function as truncal drivers in the development of CCRCC [4,16,17,19]. Mutations in *PBRM1*, *SETD2*, and *BAP1* have been identified in CCRCC and are notably located on the short arm of chromosome 3p (all within a 50-Mb region), highlighting further importance in assessing 3p mutations/deletions [14,37].

Similar to the hallmark chromosome 3p deletion in CCRCC, the study by Kovac et al describes similar evolution of PRCC from a truncal chromosomal alteration, such as trisomy chromosome 7 and/or 17, followed by subsequent subclonal mutations.[12] While types 1 and 2 PRCC have been shown to be genetically and clinically distinct, a substantial majority show chromosomal gains of 7 and 17.[38] PRCC mutations also include *MET*, *NF2* (in the Hippo signaling pathway), and *PNKD* which occur on chromosome 7 [39]. Drugs such as foretinib which is a tyrosine kinase agent targeting *MET*, *AXL*, and other receptors have been used [40]. Some evidence has been shown to suggest chemotherapeutic agents used to treat CCRCC, including sunitinib, sorafenib, and mTOR inhibitors such as everolimus and temsirolimus, also show efficacy in other RCC subtypes including PRCC and chromophobe renal cell carcinoma[41]. Interestingly, Foretinib appears to benefit patients with germline *MET* mutations compared to all PRCC patients [40].

In current models of RCC evolution and of cancer progression, prior data suggest that conventional and sarcomatoid tumor components likely arise from a common progenitor cell with subsequent subclonal populations arising as the tumor progresses.[8,9] It has been reported

that areas of sarcomatoid differentiation in RCC have increased mutations and greater loss of heterozygosity.[42] Gulati et al among other previous studies evaluating intratumoral heterogeneity, particularly at the subclonal level, have argued that single focus sampling is insufficient for true molecular classification of individual tumors.[10,43,44] Previously, Kouba et al have compared mutational variability between primary and matched metastatic lesions, which have shown similarities in a majority of tumor pairs.[21,45] Conversely, a study by Huang et al demonstrated chromosome 3p deletions in metastatic RCC that were not present in the primary tumor, which was identified in a single case within our current study.[5] Ito et al have demonstrated foci of sarcomatoid morphology or matched metastatic sites may contain high rates of chromosomal imbalances, but we have demonstrated that truncal hallmark drivers are often maintained.[6] Other histologic types of RCC, such as chromophobe RCC, have been shown to contain similar preservation of genetic abnormalities between primary and matched metastatic lesions.[46-48] Several studies have argued that metastatic lesions are less heterogeneous, but also completely different genetically, from their primary lesion.[5] Our study highlighted complete chromosomal concordance between all tumor foci within each metastatic lesion in both CCRCC and PRCC.

Overall, the 5-year survival for RCC ranges from 61–72%.[49,50] Regardless of the histologic subtype, high-stage RCC disease has a 5-year survival rate of 53% and only 8% with metastatic disease.[51] Adjuvant chemotherapy has historically been reserved for RCC patients with metastatic disease.[52,53] Ravaud et al have suggested that adjuvant treatment with high-risk nonmetastatic RCC could provide significantly longer disease-free survival.[54] VHL mutations are associated with dysregulated angiogenesis. Tyrosine kinase inhibitors, including sunitinib, sorafenib, pazopanib, axitinib, levatinib, and cabozantinib and remain first line therapy

in metastatic RCC, have been used in treatment of advanced RCCs since the early 21st century.[11,55-57] Success using these chemotherapeutic agents appears to stem from targeting activating mutations of angiogenesis by way of VEGF receptors and the MTOR[33,58,59]. Some evidence has been shown to suggest chemotherapeutic agents used to treat CCRCC, including sunitinib, sorafenib, and mTOR inhibitors such as everolimus and temsirolimus, could also show efficacy in other RCC subtypes including PRCC and chromophobe renal cell carcinoma[14,41,60]. The *VHL* gene, located on chromosome 3p25, has been shown to be a tumor suppressor gene; therefore, deletion or inactivation has been attributed to downstream effects on *HIF*. [14,61] Demonstration of preserved chromosome 3p deletions in intratumoral and metastatic foci is of importance given the first line targeted therapies in chemotherapeutic regimens. In addition to its correlation with *VHL*, chromosome 3p deletion has been attributed with better overall survival in CCRCC patients. Of note, correlating overall survival as it relates to chromosome 14q (which harbors the *HIF1A* gene) status has also been evaluated.[62]

As previously stated, studies have postulated that intratumoral heterogeneity contributes to therapeutic resistance likely secondary to intratumoral genetic heterogeneity by a combination of genomic instability and Darwinian cancer evolution.^[2,10,29] Furthermore, these studies maintain that genomic/genetic reprofiling of metastatic lesions could be a novel approach to identify causes of resistance to anti-*VEGF* inhibitors.[23] Genetic overlap between CCRCC and PRCC, upwards of 100 genes, has been described.[63] Of note, resistance to first line VEGF inhibitors has been attributed to mutations in tyrosine kinase pathways (e.g. MET or AXL). Combination therapy or use of drugs that target both VEGF and MET pathways (e.g. cabozantinib) could in theory address this issue, but toxicity with agents remains a serious issue in RCC treatment[53]. While both tumors have similar treatment modalities in the metastatic

setting, a study by Voss et al postulated that the decreased effectiveness of treatment of metastatic PRCC is likely secondary more to the use of antiangiogenic therapies in a tumor that typically lacks *VHL* loss rather than resistance secondary to tumor heterogeneity.[64]

Unfortunately, challenges in treating metastatic PRCC appear to go beyond targeting a truncal clonal chromosomal alteration (e.g., trisomy 7 or 17). While combination chemotherapeutic drugs like foretinib, a *MET/VEGF* inhibitor, may show efficacy in patients with PRCC (as the *MET* gene is located on chromosome 7), the complex genetic landscape of these tumors continually poses a challenge to treatment.[40,53,65]

Our current study has corroborated many prior molecular findings in CCRCC and PRCC, such as hallmark abnormalities and relative preservation of chromosomal status by multifocal analysis. Unfortunately, this has not elucidated why efficacy of chemotherapeutic agents is so poor. Given that mutations/alterations in CCRCC, including lesser known mutations such as *BAP1* and *SETD2*, typically occur on the short arm of 3p, current regimens targeting these regions have done little to improve overall survival and disease-free survival[14]. While we may have been able to prove that CCRCC and PRCC tumors retain similar chromosomal status regardless of tumor divergence or metastasis, this unfortunately also highlights that tumor progression likely goes beyond the pathways described above.

One potential limitation identified in this study is the ability to identify all possible chromosome 3p genetic alterations in clear cell renal cell carcinoma by FISH studies[16-19]. In the current study, the BAC clone probe used was 169K in size. According to other metaphase and molecular studies, the majority of the 3p deletions in CCRCC were in the pattern of 3p13-ptar or 3p25-pter deletion, and microdeletions were not typically reported in CCRCC [4,13,14,66,67]. Since the previously reported deletions were far greater in size than that of the

probe (169KB), we felt a vast majority would be detectable by the probe. The histograms (Figure 3G and 6E) represent the signal pattern distribution from 100 typical tumor cells from CCRCC (3G) and PRCC (6E). The x-axis represents the signal patterns and the y-axis represents the cell numbers that bearing a specific signal pattern. The 3p25 deletion histogram demonstrated that more than 60% of the tumor cells presented as 1G2R pattern (3p25 deletion). A small population of cells also showed disomic (2G2R), section truncations (1G/1R or 2G1R) or more than 3 of G/R signals, which may represent the DNA replication in the population of mitotic cells. For the chromosome 7/17 enumeration, the histogram showed that about 80% of cells demonstrated trisomy (all populations with 3G signal pattern, while the chromosome 17 trisomy frequency was about 70% of total tumor cell populations. The histogram shows that the current threshold could effectively detect the chromosome deletion and gains.

While a majority of allelic loss occurs by simple deletion, a subset of tumors have been shown to incur loss of chromosome region by uniparental disomy (UPD) or copy-neutral loss of heterozygosity (LOH)[68]. Traditionally UPD, which occurs when a person inherits two chromosomal copies from the same parent and none from the other, had been associated with inherited-type diseases [18,69]. However, prior studies have shown this can occur in an acquired fashion in hematopoietic and solid organ malignancies [70-72]. Unfortunately, these LOH or copy number-neutral changes could not be detectable by current FISH platforms, despite using a BAC clone probe (RP11-572M14, chr3: 10,011,785-10,180,797) that covers the entire sequence of VHL gene (VHL, chr3:10,141,008-10,153,670) [16,17,25,26,69,73]. Further molecular analysis, particularly by high-resolution single-nucleotide polymorphism microarrays, may serve to identify an even higher percentage of alterations in 3p chromosomal regions in future studies [8,16,17,26,68].

RCC with sarcomatoid features is an aggressive, heterogeneous subset of tumors that frequently present at a high clinical stage. We evaluated 387 tumor foci of 58 separate RCCs within conventional, sarcomatoid, and metastatic components. Overall, our study demonstrates impressive preservation of chromosomal status across multiple sampled foci within similar tumor components as well as comparatively between divergent morphologies and in the metastatic setting. While concordance of chromosomal status was preserved in a majority of cases, we did identify heterogeneity in a subset. Further study of tumor heterogeneity, particularly at the subclonal level, may offer vital information in an age of targeted therapy where efficacy remains suboptimal.

Acknowledgements: The authors would like to thank Natasha Gibson for excellent editorial assistance.

References:

1. McGranahan N, Swanton C. Clonal heterogeneity and tumor evolution: past, present, and the future. *Cell* 2017;168:613-628.
2. Andor N, Graham TA, Jansen M et al. Pan-cancer analysis of the extent and consequences of intratumor heterogeneity. *Nat Med* 2016;22:105-113.
3. Gerlinger M, Rowan AJ, Horswell S et al. Intratumor heterogeneity and branched evolution revealed by multiregion sequencing. *N Engl J Med* 2012;366:883-892.
4. Gerlinger M, Horswell S, Larkin J et al. Genomic architecture and evolution of clear cell renal cell carcinomas defined by multiregion sequencing. *Nat Genet* 2014;46:225-233.
5. Huang Y, Gao S, Wu S et al. Multilayered molecular profiling supported the monoclonal origin of metastatic renal cell carcinoma. *Int J Cancer* 2014;135:78-87.
6. Ito T, Pei J, Dulaimi E et al. Genomic copy number alterations in renal cell carcinoma with sarcomatoid features. *J Urol* 2016;195:852-858.
7. de Peralta-Venturina M, Moch H, Amin M et al. Sarcomatoid differentiation in renal cell carcinoma: a study of 101 cases. *Am J Surg Pathol* 2001;25:275-284.
8. Jones TD, Eble JN, Wang M, Maclennan GT, Jain S, Cheng L. Clonal divergence and genetic heterogeneity in clear cell renal cell carcinomas with sarcomatoid transformation. *Cancer* 2005;104:1195-1203.
9. Malouf GG, Ali SM, Wang K et al. Genomic characterization of renal cell carcinoma with sarcomatoid dedifferentiation pinpoints recurrent genomic alterations. *Eur Urol* 2016;70:348-357.
10. Gerlinger M, Swanton C. How Darwinian models inform therapeutic failure initiated by clonal heterogeneity in cancer medicine. *Br J Cancer* 2010;103:1139-1143.

11. Brunelli M, Fiorentino M, Gobbo S et al. Many facets of chromosome 3p cytogenetic findings in clear cell renal carcinoma: the need for agreement in assessment FISH analysis to avoid diagnostic errors. *Histol Histopathol* 2011;26:1207-1213.
12. Kovac M, Navas C, Horswell S et al. Recurrent chromosomal gains and heterogeneous driver mutations characterise papillary renal cancer evolution. *Nat Commun* 2015;6:6336.
13. The Cancer Genome Atlas Network. Comprehensive molecular characterization of clear cell renal cell carcinoma. *Nature* 2013;499:43-49.
14. Frew IJ, Moch H. A clearer view of the molecular complexity of clear cell renal cell carcinoma. *Annu Rev Pathol* 2015;10:263-289.
15. The Cancer genome Atlas Network. Comprehensive molecular characterization of papillary renal-cell carcinoma. *N Engl J Med* 2016;374:135-145.
16. Cheng L, Zhang S, Wang L, MacLennan GT, Davidson DD. Fluorescence in situ hybridization in surgical pathology: principles and applications. *J Pathol Clin Res* 2017;3:73-99.
17. Cheng L, Zhang S, MacLennan GT, Lopez-Beltran A, Montironi R. Molecular and cytogenetic insights into the pathogenesis, classification, differential diagnosis, and prognosis of renal epithelial neoplasms. *Human pathology* 2009;40:10-29.
18. Cheng LZ, DY.; Eble, JN. *Molecular Genetic Pathology*. New York, NY: Springer; 2013.
19. Cheng L, Eble JN. *Molecular Surgical Pathology*. New York, NY: Springer; 2013.
20. Cheng L, Williamson SR, Zhang S, MacLennan GT, Montironi R, Lopez-Beltran A. Understanding the molecular genetics of renal cell neoplasia: implications for diagnosis, prognosis and therapy. *Expert review of anticancer therapy* 2010;10:843-864.

21. Kouba EJ, Eble JN, Simper N et al. High fidelity of driver chromosomal alterations among primary and metastatic renal cell carcinomas: implications for tumor clonal evolution and treatment. *Mod Pathol* 2016;29:1347-1357.
22. Wang L, Williamson SR, Wang M et al. Molecular subtyping of metastatic renal cell carcinoma: implications for targeted therapy. *Mol Cancer* 2014;13:39.
23. Massari F, Ciccicarese C, Bria E et al. Reprofileing metastatic samples for chromosome 9p and 14q aberrations as a strategy to overcome tumor heterogeneity in clear-cell renal cell carcinoma. *Appl Immunohistochem Mol Morphol* 2017;25:39-43.
24. Moch H, Humphrey PA, Ulbright TM, Reuter VE. WHO classification of tumors of the urinary system and male genital organ. Lyon: LARC Press; 2016.
25. Jones TD, Eble JN, Wang M et al. Molecular genetic evidence for the independent origin of multifocal papillary tumors in patients with papillary renal cell carcinomas. *Clin Cancer Res* 2005;11:7226-7233.
26. Cheng L, MacLennan GT, Zhang S et al. Evidence for polyclonal origin of multifocal clear cell renal cell carcinoma. *Clin Cancer Res* 2008;14:8087-8093.
27. Halat S, Eble JN, Grignon DJ et al. Multilocular cystic renal cell carcinoma is a subtype of clear cell renal cell carcinoma. *Mod Pathol* 2010;23:931-936.
28. McGranahan N, Swanton C. Biological and therapeutic impact of intratumor heterogeneity in cancer evolution. *Cancer Cell* 2015;27:15-26.
29. Burrell RA, Swanton C. Re-evaluating clonal dominance in cancer evolution. *Trends Cancer* 2016;2:263-276.
30. Bi M, Zhao S, Said JW et al. Genomic characterization of sarcomatoid transformation in clear cell renal cell carcinoma. *Proc Natl Acad Sci U S A* 2016;113:2170-2175.

31. Venkatesan S, Swanton C. Tumor evolutionary principles: How intratumor heterogeneity influences cancer treatment and outcome. *Am Soc Clin Oncol Educ Book* 2016;35:e141-149.
32. Hsieh JJ, Manley BJ, Khan N, Gao J, Carlo MI, Cheng EH. Overcome tumor heterogeneity-imposed therapeutic barriers through convergent genomic biomarker discovery: A braided cancer river model of kidney cancer. *Semin Cell Dev Biol* (2016, in press).
33. Hsieh JJ, Purdue MP, Signoretti S et al. Renal cell carcinoma. *Nat Rev Dis Primers* 2017;3:17009.
34. Schwartz R, Schaffer AA. The evolution of tumour phylogenetics: principles and practice. *Nat Rev Genet* 2017;advance online publication.
35. McDonald O, Li X, Saunders T et al. Epigenomic reprogramming during pancreatic cancer progression links anabolic glucose metabolism to distant metastasis. *Nat Genet* (2017, In press).
36. Semenza GL. HIF-1 mediates metabolic responses to intratumoral hypoxia and oncogenic mutations. *J Clin Invest* 2013;123:3664-3671.
37. Cohen HT, McGovern FJ. Renal-cell carcinoma. *N Engl J Med* 2005;353:2477-2490.
38. The Cancer Genome Atlas Research Network. Comprehensive molecular characterization of papillary renal-cell carcinoma. *N Engl J Med* 2016;374:135-145.
39. Gonzalez Del Alba A, Arranz JA, Puente J et al. Recent advances in genitourinary tumors: A review focused on biology and systemic treatment. *Crit Rev Oncol Hematol* 2017;113:171-190.

40. Choueiri TK, Vaishampayan U, Rosenberg JE et al. Phase II and biomarker study of the dual MET/VEGFR2 inhibitor foretinib in patients with papillary renal cell carcinoma. *J Clin Oncol* 2013;31:181-186.
41. Abbosh P, Sundararajan S, Millis S et al. Molecular and genomic profiling to identify actionable targets in chromophobe renal cell cancer. *Eur Urol Focus* 2017;(in press).
42. Manley BJ, Hsieh JJ. Sarcomatoid renal cell carcinoma: genomic insights from sequencing of matched sarcomatous and carcinomatous components. *Transl Cancer Res* 2016:S160-S165.
43. Gulati S, Martinez P, Joshi T et al. Systematic evaluation of the prognostic impact and intratumour heterogeneity of clear cell renal cell carcinoma biomarkers. *Eur Urol* 2014;66:936-948.
44. Haddad AQ, Margulis V. Tumour and patient factors in renal cell carcinoma-towards personalized therapy. *Nat Rev Urol* 2015;12:253-262.
45. Goswami RS, Patel KP, Singh RR et al. Hotspot mutation panel testing reveals clonal evolution in a study of 265 paired primary and metastatic tumors. *Clin Cancer Res* 2015;21:2644-2651.
46. Brunelli M, Gobbo S, Cossu-Rocca P et al. Chromosomal gains in the sarcomatoid transformation of chromophobe renal cell carcinoma. *Mod Pathol* 2007;20:303-309.
47. Abbosh P, Sundararajan S, Millis S et al. Molecular and genomic profiling to identify actionable targets in chromophobe renal cell cancer. *Eur Urol Focus* (2017, in press).
48. Davis CF, Ricketts CJ, Wang M et al. The somatic genomic landscape of chromophobe renal cell carcinoma. *Cancer Cell* 2014;26:319-330.

49. Znaor A, Lortet-Tieulent J, Laversanne M, Jemal A, Bray F. International variations and trends in renal cell carcinoma incidence and mortality. *Eur Urol* 2015;67:519-530.
50. Capitanio U, Montorsi F. Renal cancer. *The Lancet*;387:894-906.
51. Siegel RL, Miller KD, Jemal A. Cancer statistics, 2017. *CA Cancer J Clin* 2017;67:7-30.
52. Gore ME, Szczylik C, Porta C et al. Final results from the large sunitinib global expanded-access trial in metastatic renal cell carcinoma. *Br J Cancer* 2015;113:12-19.
53. Choueiri TK, Motzer RJ. Systemic therapy for metastatic renal-cell carcinoma. *N Engl J Med* 2017;376:354-366.
54. Ravaud A, Motzer RJ, Pandha HS et al. Adjuvant sunitinib in high-risk renal-cell carcinoma after nephrectomy. *N Engl J Med* 2016;375:2246-2254.
55. Motzer RJ, Hutson TE, Cella D et al. Pazopanib versus sunitinib in metastatic renal-cell carcinoma. *N Engl J Med* 2013;369:722-731.
56. Escudier B, Porta C, Schmidinger M et al. Renal cell carcinoma: ESMO clinical practice guidelines for diagnosis, treatment and follow-up. *Ann Oncol* 2016;27:v58-v68.
57. Haas NB, Manola J, Uzzo RG et al. Adjuvant sunitinib or sorafenib for high-risk, non-metastatic renal-cell carcinoma (ECOG-ACRIN E2805): a double-blind, placebo-controlled, randomised, phase 3 trial. *Lancet* 2016;387:2008-2016.
58. Yap TA, Gerlinger M, Futreal PA, Pusztai L, Swanton C. Intratumor heterogeneity: seeing the wood for the trees. *Sci Transl Med* 2012;4:127ps110.
59. Zhang J, Yang PL, Gray NS. Targeting cancer with small molecule kinase inhibitors. *Nat Rev Cancer* 2009;9:28-39.

60. Buchler T, Bortlicek Z, Poprach A et al. Outcomes for patients with metastatic renal cell carcinoma achieving a complete response on targeted therapy: a registry-based analysis. *Eur Urol* 2016;70:469-475.
61. Klatter T, Rao PN, de Martino M et al. Cytogenetic profile predicts prognosis of patients with clear cell renal cell carcinoma. *J Clin Oncol* 2009;27:746-753.
62. Kroeger N, Klatter T, Chamie K et al. Deletions of chromosomes 3p and 14q molecularly subclassify clear cell renal cell carcinoma. *Cancer* 2013;119:1547-1554.
63. Chen F, Zhang Y, Senbabaoglu Y et al. Multilevel genomics-based taxonomy of renal cell carcinoma. *Cell Rep* 2016;14:2476-2489.
64. Voss MH, Molina AM, Chen YB et al. Phase II Trial and Correlative Genomic Analysis of Everolimus Plus Bevacizumab in Advanced Non-Clear Cell Renal Cell Carcinoma. *J Clin Oncol* 2016;34:3846-3853.
65. Albiges L, Guegan J, Le Formal A et al. MET is a potential target across all papillary renal cell carcinomas: result from a large molecular study of pRCC with CGH array and matching gene expression array. *Clin Cancer Res* 2014;20:3411-3421.
66. Beuselinck B, Job S, Becht E et al. Molecular subtypes of clear cell renal cell carcinoma are associated with sunitinib response in the metastatic setting. *Clin Cancer Res* 2015;21:1329-1339.
67. Fenner A. Genetics: a molecular atlas of clear cell renal cell carcinoma. *Nat Rev Clin Oncol* 2013;10:485.
68. Sato Y, Yoshizato T, Shiraishi Y et al. Integrated molecular analysis of clear-cell renal cell carcinoma. *Nat Genet* 2013;45:860-867.

69. Saeki H, Kitao H, Yoshinaga K et al. Copy-neutral loss of heterozygosity at the p53 locus in carcinogenesis of esophageal squamous cell carcinomas associated with p53 mutations. *Clin Cancer Res* 2011;17:1731-1740.
70. Murthy SK, DiFrancesco LM, Ogilvie RT, Demetrick DJ. Loss of heterozygosity associated with uniparental disomy in breast carcinoma. *Mod Pathol* 2002;15:1241-1250.
71. Andersen CL, Wiuf C, Kruhoffer M, Korsgaard M, Laurberg S, Orntoft TF. Frequent occurrence of uniparental disomy in colorectal cancer. *Carcinogenesis* 2007;28:38-48.
72. Ogiwara H, Kohno T, Nakanishi H, Nagayama K, Sato M, Yokota J. Unbalanced translocation, a major chromosome alteration causing loss of heterozygosity in human lung cancer. *Oncogene* 2008;27:4788-4797.
73. Castronovo C, Valtorta E, Crippa M et al. Design and validation of a pericentromeric BAC clone set aimed at improving diagnosis and phenotype prediction of supernumerary marker chromosomes. *Molecular cytogenetics* 2013;6:45.

Figure Legends

Figure 1. Sampling of tumor foci for fluorescence in situ hybridization (FISH) studies. **(A)** Primary renal cell carcinoma tumors were sampled to identify three separate tumor foci in conventional regions and three additional foci in sarcomatoid regions for FISH. Additionally, three tumor foci were marked for FISH analysis in each matched metastatic sites including lymph node, bone, brain, and lung.

Figure 2. Chromosome 3p status in primary clear cell renal cell carcinoma (including conventional and sarcomatoid tumor foci) with matched metastatic sites. **(A)** Overall chromosome 3p status including concordant and discordant chromosome 3p deletions as well as clear cell renal carcinoma with no deletion of chromosome 3p. **(B-C)** Sarcomatoid and conventional clear cell renal carcinoma morphologies with concordant (all foci) and discordant (1 or 2 of 3 foci) deletions of chromosome 3p. A subset with no deletion of chromosome 3p in any focus was identified in both morphologies. **(D)** Concordant deletion (all tumor foci) of chromosome 3p in all matched metastatic sites was identified in 10 of 11 cases.

Figure 3. Primary clear cell renal cell carcinoma (CCRCC), sarcomatoid and conventional morphologies. **(A-B)** Transition between conventional and sarcomatoid morphologies, low power **(A)** and high power **(B)**. **(C)** CCRCC with sarcomatoid features with loss of chromosome 3p using interphase fluorescence in situ hybridization (FISH; see inset). **(D)** Sarcomatoid CCRCC with no deletion of chromosome 3p (see inset). **(E)** Conventional CCRCC with loss of chromosome 3p by FISH (see inset). **(F)** Conventional CCRCC with no deletion of chromosome 3p (see inset). **(G)** Histogram of FISH signal distribution of a typical CCRCC. G: Green signal

corresponding 3p25; R: Red signal corresponding to CEP3. Vertical axis represents the percentage of cells showing the specific signal pattern, The signal pattern was denominated as #G#R, which present as number of Green signal (3p25) and number of Red signal (CEP3).

Figure 4. Primary clear cell renal cell carcinoma (CCRCC; conventional and sarcomatoid, multiple foci) with matched metastatic sites. **(A)** CCRCC with sarcomatoid features with chromosomal 3p deletion in two of three foci using interphase fluorescence in situ hybridization (FISH). **(B)** Conventional CCRCC with chromosomal 3p deletion in two of three foci by FISH. **(C)** Matched metastatic CCRCC to lung, 7 years status post nephrectomy, with chromosomal 3p deletion by FISH. **(D)** Matched metastatic CCRCC to brain, 11 years status post nephrectomy, with chromosomal 3p deletion by FISH.

Figure 5. Chromosome 7 and 17 statuses in papillary renal cell carcinoma (PRCC; including conventional and sarcomatoid tumor foci) with matched metastatic sites. **(A)** Overall, all six PRCC carcinoma tumors demonstrated trisomy 7 and 17 in conventional and sarcomatoid tumor foci. **(B-C)** Trisomy 7 and 17 was identified in single tumor focus in both the sarcomatoid and conventional sampling demonstrating minor discordance. **(D)** Matched metastatic PRCC demonstrated trisomy 7 and 17 in concordance with the primary lesions.

Figure 6. Primary (conventional and sarcomatoid) and matched metastatic papillary renal cell carcinoma (PRCC). **(A)** Transition between conventional and sarcomatoid PRCC, low power. **(B)** Sarcomatoid PRCC, multiple foci, with trisomy 7 and 17 using interphase fluorescence in situ hybridization (FISH; inset). **(C)** Conventional PRCC, multiple foci, with trisomy 7 and 17

using FISH (inset). **(D)** Matched metastatic PRCC with trisomy 7 and 17 by FISH (inset). **(E)** Histogram of Chromosome 7/17 FISH signal representing a typical PRCC. G: Green signal corresponding CEP17; R: Red signal corresponding to CEP7. Vertical axis represents the percentage of cells showing the specific signal pattern, which was denominated as #G#R, which present as number of Green signal (CEP17) and number of Red signal (CEP7).

Table 1. Demographics and Histopathologic Features

	Age (years)	Male to Female Ratio (M:F)	Tumor Size (mm)	Sarcomatoid Features (range, %)	Pathologic Stage (pT) at Diagnosis (when available)	Metastatic Samples Available for Molecular Analysis
Clear Cell Renal Cell Carcinoma (n = 52)	57 (mean) 28 – 76 (range)	1.3 : 1.0	106 (mean) 43 to 205 (range)	< 5 to 90%	pT1 = 3 pT2 = 3 pT3 = 32 pT4 = 4	n = 11 (15%) bone, brain, gastrointestinal, liver, lymph node, and lung
Papillary Renal Cell Carcinoma (n = 6)	54 (mean) 28 – 77 (range)	5.0 : 1.0	71 (mean) 20 to 150 (range)	<5 to 60%	pT1 = 1 pT2 = 2 pT3 = 3	n = 2 (33%) Small bowel and lung

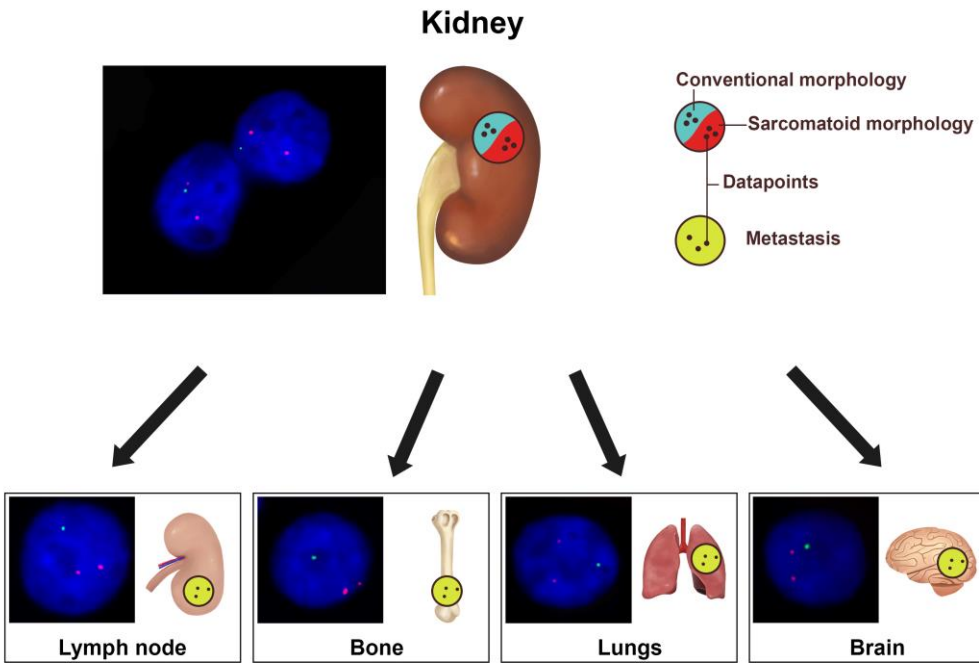


Figure 1

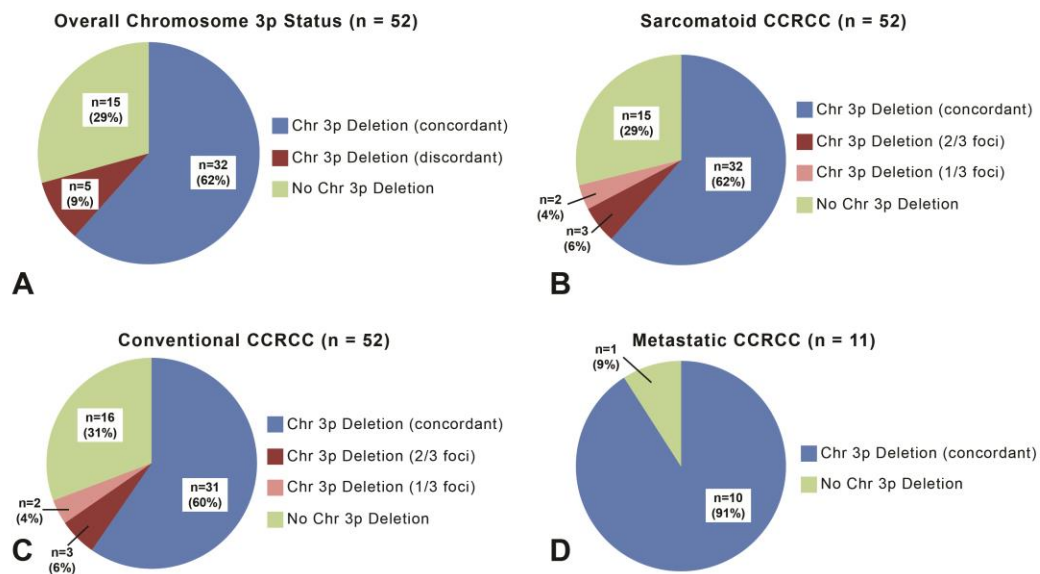


Figure 2

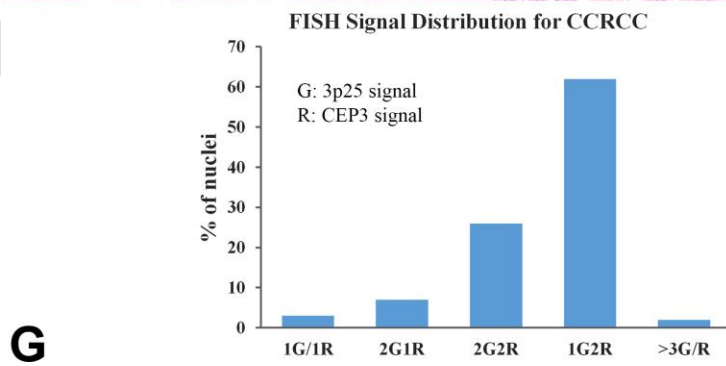
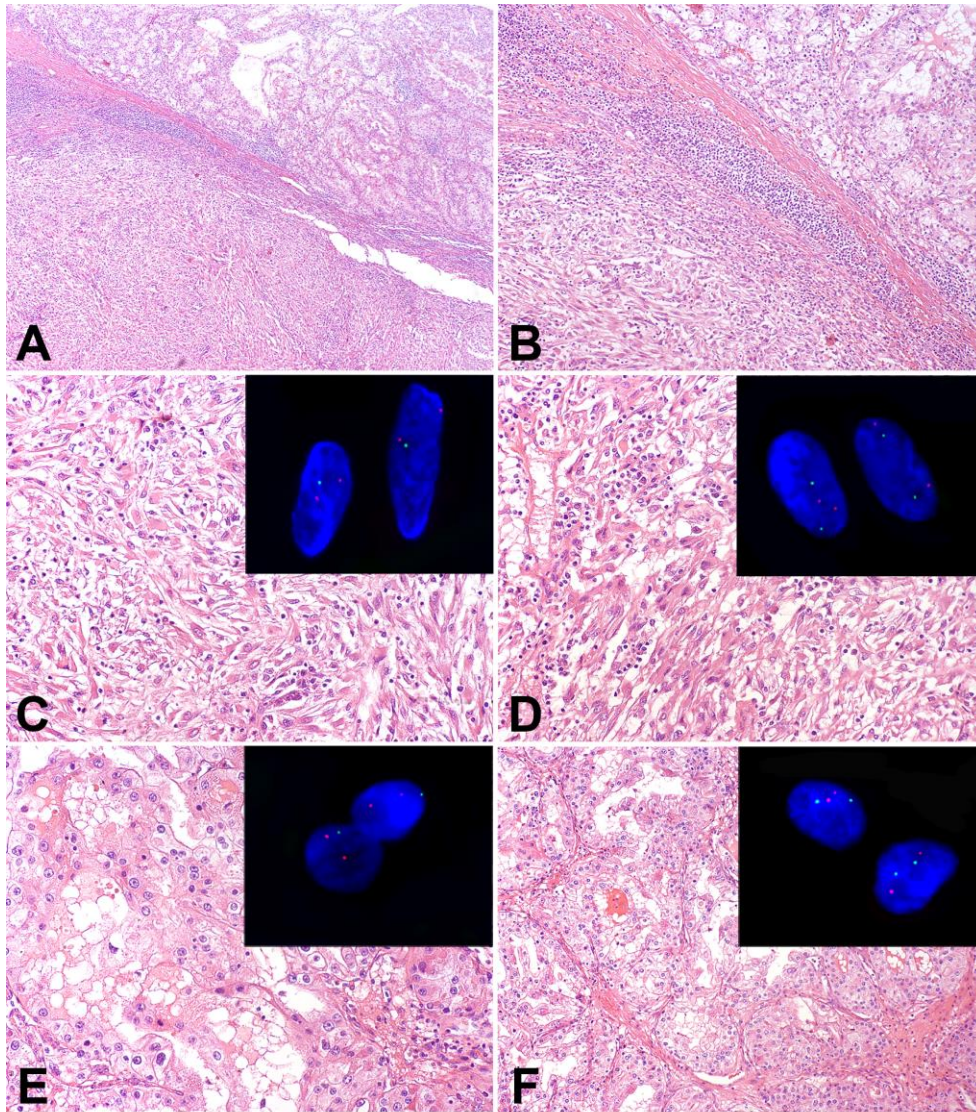


Figure 3

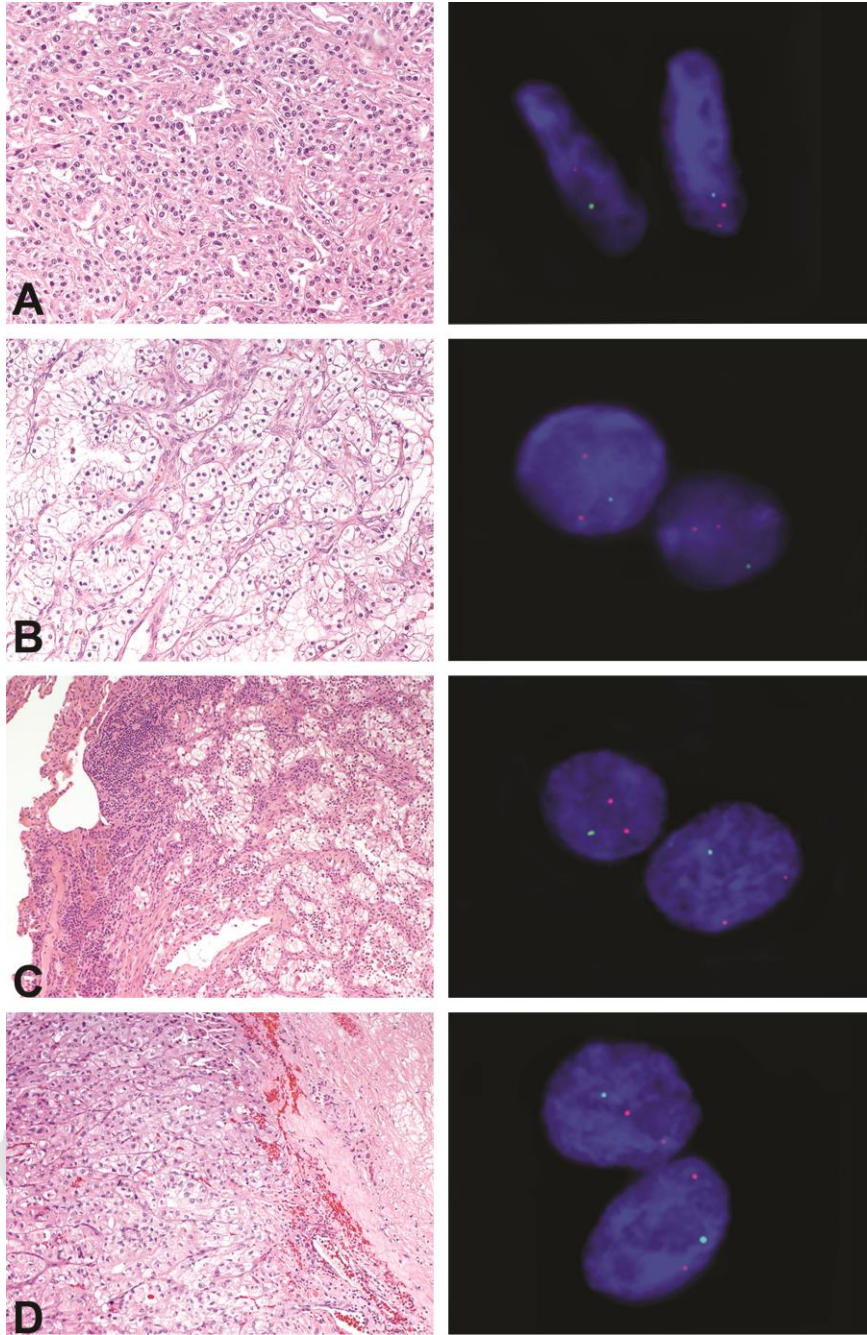


Figure 4

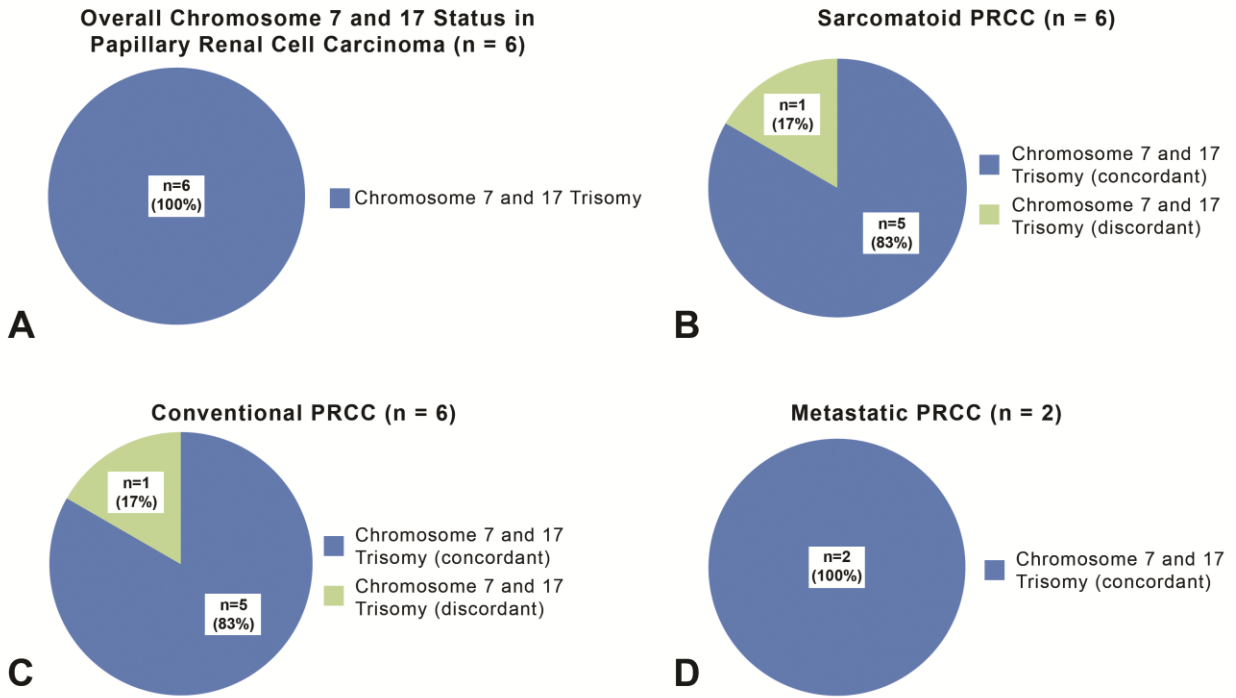
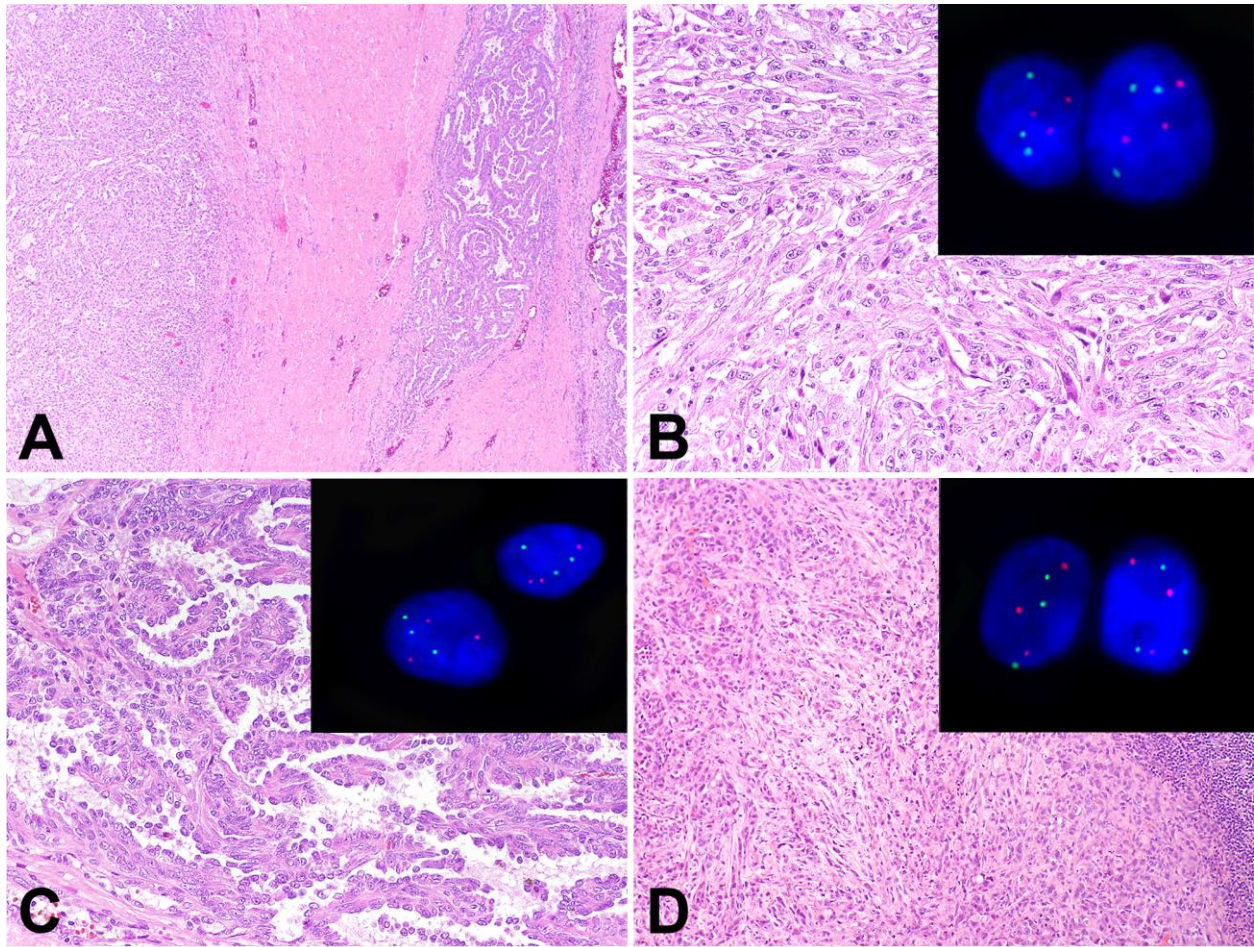


Figure 5



E

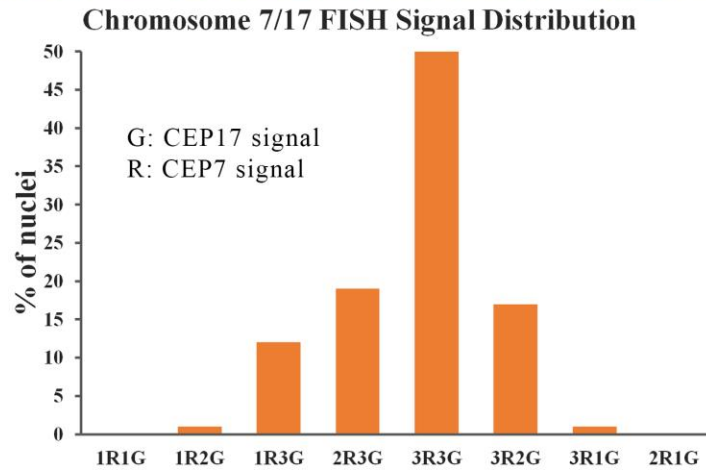


Figure 6